Fachtagung "Lasermethoden in der Strömungsmesstechnik"
3. – 5. September 2013, München

Bestimmung von Geschwindigkeitsprofilen in engen Spalten paralleler, ebener Glasscheiben mit Hilfe tomografischer PIV-Messtechnik

Determination of velocity profiles in small gaps between parallel flat plates by means of tomographic PIV

Constantin Schosser*, Rainer Hain, Christian Cierpka**, Stefan Lecheler*, Christian J. Kähler**, Michael Pfitzner*****

* Universität der Bundeswehr München, Fakultät Maschinenbau, Technische Thermodynamik
Werner-Heisenberg-Weg 39, 85577 Neubiberg
E-Mail: Constantin.Schosser@unibw.de

** Universität der Bundeswehr München, Fakultät für Luft- und Raumfahrttechnik, Institut für Strömungsmechanik und Aerodynamik
Werner-Heisenberg-Weg 39, 85577 Neubiberg

*** Universität der Bundeswehr München, Fakultät für Luft- und Raumfahrttechnik, Institut für Thermodynamik
Werner-Heisenberg-Weg 39, 85577 Neubiberg

Tomografische PIV, PTV, Geschwindigkeitsprofil, Tesla Turbine, Reibungsturbine
Tomographic PIV, PTV, velocity profile, Tesla turbine, friction-type turbine

Abstract

A flow between two parallel, flat and non-rotating glass-plates with a gap of 1 mm has been examined, applying the tomographic PIV measurement technique. The fluid applied for the measurements was dried and compressed air at ambient temperature. Several modifications have been tested to achieve a suitable illumination of the particles to be tracked. In addition, different calibration-targets have been tested. In order to verify the results by measuring a parabolic velocity profile, the fluid velocity has been set to values suitable for laminar flow conditions (Re < 2800 for rectangular cross-sections with high aspect ratios). Two time-dependent volumes with particles were analyzed from double-frame images of both cameras using the DaVis 8.1.3 software. Data from these volumes were processed in Matlab. A particle tracking code is then used to calculate the particle displacements. The measurements are done in preparation for PIV-measurements between two parallel, corotating disks in a future test rig of a Tesla turbine / friction-type turbine. The aim of the analysis of a Tesla turbine is the experimental verification of numerical simulations (CFD). These preliminary studies provide information for the design of a suitable Tesla turbine test-rig. This test also demonstrates the applicability PIV measurement technique to the application and in general to flows in small gaps.

Introduction

Nikola Tesla's turbo machinery was patented in 1913. A Tesla turbine's rotor consists of several corotating disks mounted on a hollow shaft. The flow driven by a pressure difference across the disc gaps enters the rotor through guide vanes at the outer radius of the disks and flows spirally towards the axis of rotation, where the flow leaves the turbine via a hollow shaft. The momentum exchange between rotor and fluid creates torque and thus power. The simple and robust design and the scalability of the design might offer an economical alternative to conventional turbo machinery, when only small quantities or individual solutions are required. This type of turbine might especially become interesting for regenerative, local power generation, provided that turbine efficiency can be proven to be reasonable.

In the 60s and 70s of the 20th century, the principle was investigated theoretically and experimentally, but practical design criteria are still missing. There is only one known experimental investigation of the velocity profiles in a Tesla turbine by Nendl 1976. Due to the fact that these studies were carried out using a wide gap width of 7 mm, while typical Tesla turbine applications need widths of 1 mm and below, the relevance of the results is limited. In addition, the hotwire measurements only offered up to 20 measurement points and influenced the flow field with their high blockage of the gap. All other known measurements in friction-type turbines only take technical characteristics like revolutions per minute, torque, power, mass flow and pressure drop into account. Efficiency and power of Tesla turbines are widely discussed, while the results from previous investigations are contradictory. In recent years, several papers showing CFD results only were published, lacking comparisons with experimental results. It is the aim of the present research to provide validation data applying state-of-the-art laser-optical measurement techniques.

Experimental set-up

The measuring section is directly connected to the seeding generator, which is fed by compressed air at ambient temperature flowing through a pressure reducing valve. The flow enters the rectangular cross section through an adapter interfacing with an air pipe. The cross section of the channel has dimensions of 75 mm x 1 mm. A measuring position 200 mm downstream of the inlet ensures a fully developed velocity profile between the two plates. Ambient pressure is applied at the outlet of the channel.

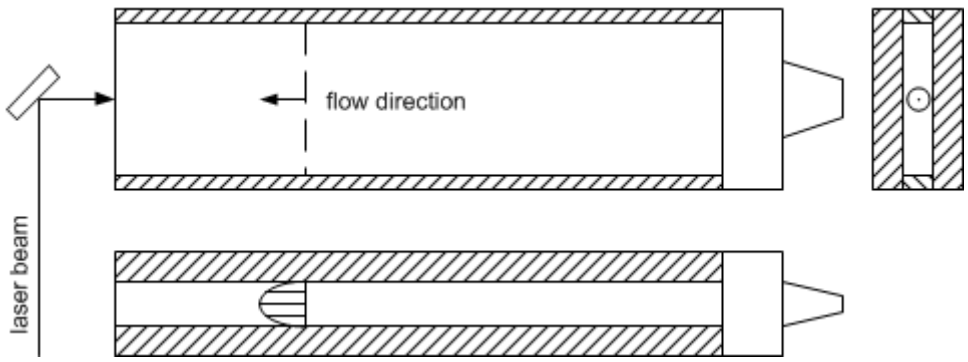

Fig. 1: Measuring section illuminated by a laser beam

The flow velocity is set to values suitable for laminar flow condition in order to have an exact solution which is available from theory (namely a parabolic velocity profile). For rectangular cross sections with aspect ratios *a* > 10 Schlichting and Gersten 2006 and Hanks and Ruo 1966 proposed a critical Reynolds number of

$$Re_{crit} = \frac{\bar{u} \cdot d_h}{v(p,T)} > 2800 \quad (1)$$

The hydraulic diameter is given by Schade and Kunz 1980 as

$$d_h = \frac{4A}{U} \quad (2)$$

where *A* is the area and *U* denotes the circumference of the cross section. At ambient pressure *p* and temperature *T* the critical velocity is

$$\bar{u}_{crit} \approx 23 m/s \quad (3)$$

In this study, the maximum velocity is set to values far below the critical velocity $\bar{u}_{crit}$.

The two cameras used in this study are LaVision Imager sCMOS. Each camera is equipped with a Scheimpflug mounting and two 2x teleconverters in combination with a 100 mm macro lens with a maximum aperture of $f_\# = 2$ are used.

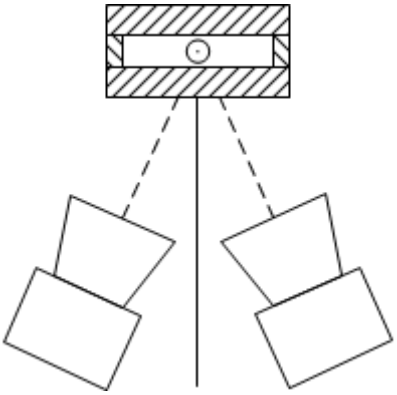

Fig. 2: Camera positions relative to the measuring section

The software DaVis 8.1.3 was used for controlling the hardware (cameras, laser) and for some steps of the data evaluation. An Innolas Spitlight 400 laser was applied for particle illumination. To adjust the focal point of the laser, the distance between a -50 mm and a +75 mm spherical lens was adapted. Several mirrors were used to position the laser beam to its defined position in the gap. The focal point was placed before the beam enters the gap, because an expanding beam ensures the illumination of the whole gap. DEHS particles from the seeding generator had an average diameter of 1 µm.

Calibration

Several calibration targets (fig. 3) were printed on a standard laser printer, glued on an object slide and finally mounted on a micrometer screw in order to vary its position during the calibration procedure. Different calibration targets have been tested. On closer examination the

target with diameter *d* = 0.3 mm and distance between the points *a* = 1 mm was too inaccurate, due to object size and limited resolution of the printer. The other two targets, shown in Fig. 3 were accepted by DaVis 8.1.3 for calibration, the resolution of these two printouts thus was satisfactory. Target *d* = 0.5 mm / *a* = 1.5 mm was chosen for further analysis, because of the larger number of calibration points.

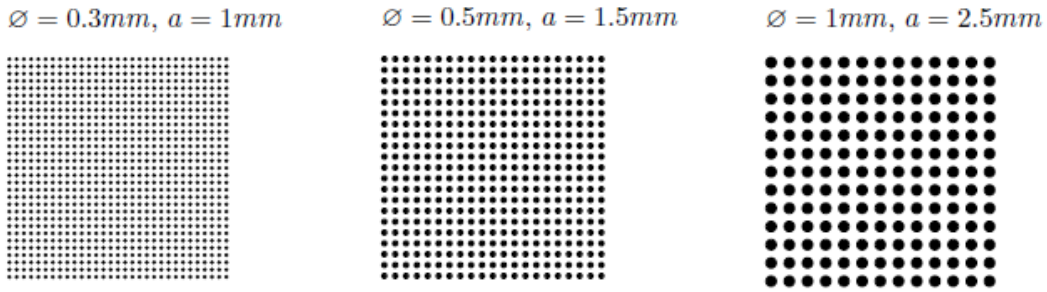

Fig. 3: Calibration targets

For a valid calibration DaVis needs two different target positions. In order to increase the accuracy of the calibration, three locations were applied at distances from the wall chosen in steps of 0.5 mm. The calibration target need always be parallel to the front glass-plate. To fulfill these requirements, the rear glass plate had to be removed for calibration. The clue ensures the same position of the front plate before and after calibration. An arrester at the front plate performs this task.

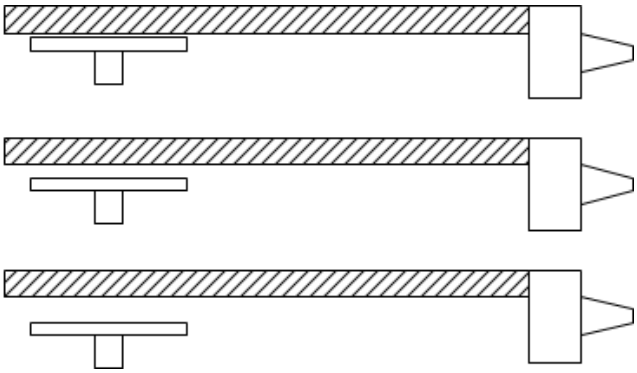

Fig. 4: Three positions of the target during calibration

Another difficulty is to ensure the zero-millimeter-position of the calibration target. There will always be a tiny gap between the front glass plate and the target. Relative to that position the two other positions 0.5 mm and 1.0 mm are precise. As it can be seen in Fig. 17, the tiny gap is visible as an offset in the position of the near wall velocities.

Recording and processing images

350 double-frame images are recorded with each camera with the LaVision software DaVis 8.1.3. In order to improve the quality of the pictures, image processing is necessary. Stabilizing the bouncing images, suppressing the reflections by subtracting averaged images, applying non-linear filters and setting the unlit background to a light intensity of zero using a threshold are the most important tools to prepare the images for the volume reconstruction.

From these batch-edited raw images DaVis tomographically reconstructed 350 “double volumes” with the fast M.A.R.T. algorithm. Due to the relatively low particle image density two cameras were sufficient for the tomographic reconstruction. The computation time for these volumes containing light intensity values for each voxel was about 24 hours with two Intel i7 quad-core cpu’s. The low particle image densities lead to a low density of “particles” (intensity spots) in the reconstructed volume. Thus, it was not reasonable to perform a conventional Tomo-PIV evaluation with correlation of interrogation volumes as this would require large interrogation volumes which here would lead to a low spatial resolution. In order to obtain a high spatial resolution, particle tracking was performed with the code described in Cierpka and Kähler 2012. To do this, the volumes had to be read in Matlab and the light intensity values were fitted in each spatial direction with a 1D Gauss algorithm. The particle positions found in each volume were used as an input for the tracking algorithm, which processed the displacement of particles. With the time step between the reconstructed volumes a velocity could be obtained for each single particle.

Measurement results and discussion

Some measurements results are given in the following. The parabolic velocity profiles in each figure are fitted from single shot measurements. The displacement limits (parameters in the tracking algorithm) of the tracked particles are -0.10 mm and 0.20 mm in *x*-direction and -0.01 mm and 0.01 mm in *y*- and *z*-direction. The time step between the double-frame images of each camera was Δt = 10 µs.

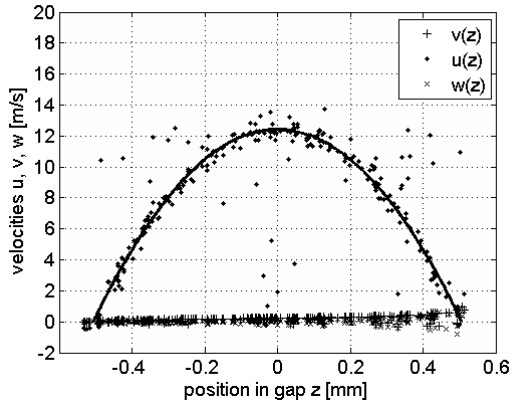

Fig. 5: Snapshot flow field no. 1/350

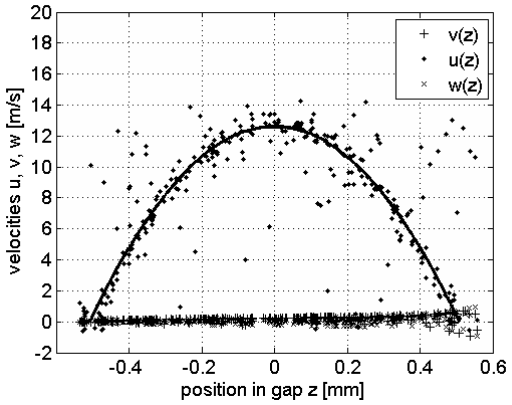

Fig. 6: Snapshot flow field no. 10/350

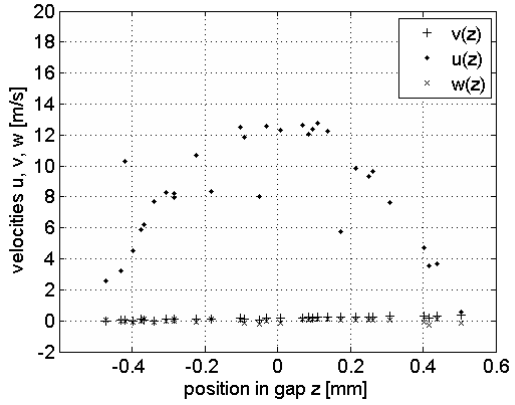

Fig. 7: Snapshot flow field no. 27/350

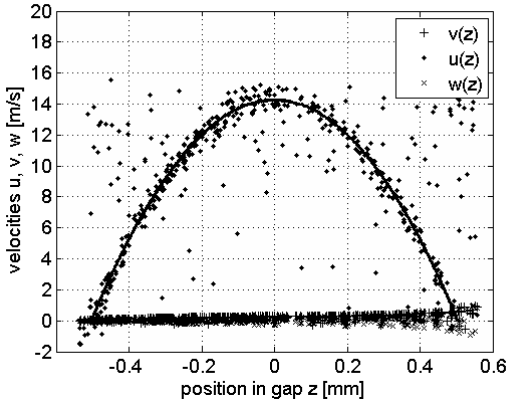

Fig. 8: Snapshot flow field no. 181/350

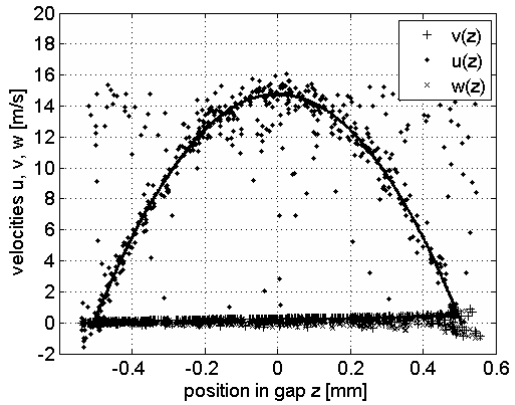

Fig. 9: Snapshot flow field no. 245/350

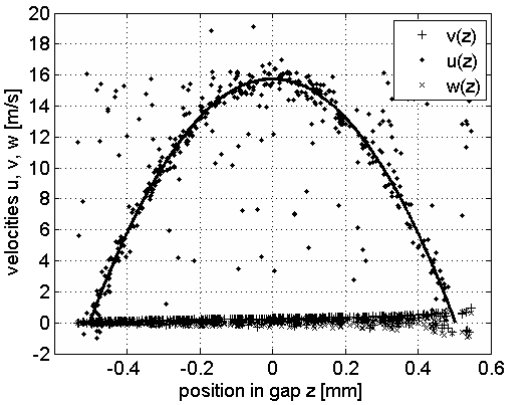

Fig. 10: Snapshot flow field no. 322/350

The following measurement results show multiple snapshots in each figure, which then are fitted by a parabolic function.

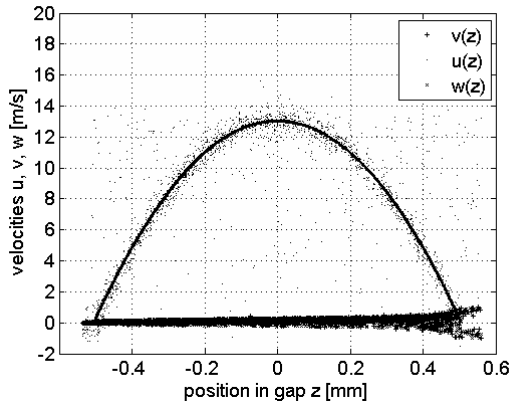

Fig. 11: Fitted from 10 snapshots (no. 60-69)

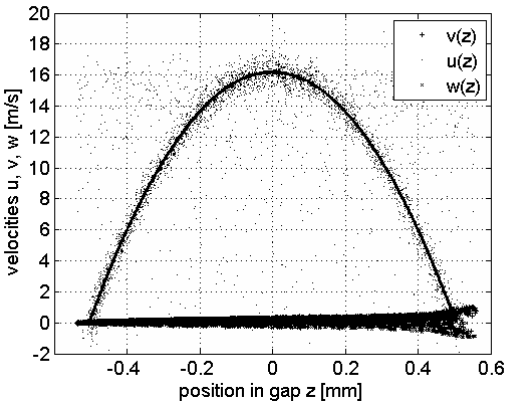

Fig. 12: Fitted from 10 snapshots (no. 340-349)

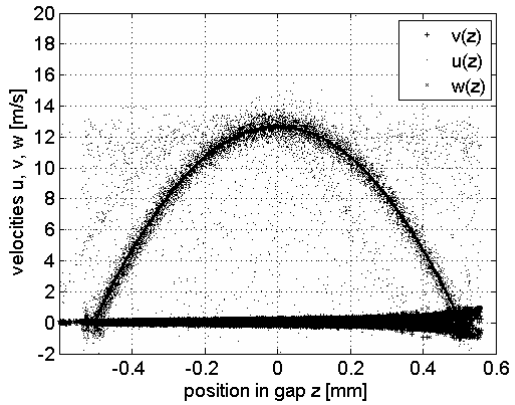

Fig. 13: Fitted from 50 snapshots (no. 1-50)

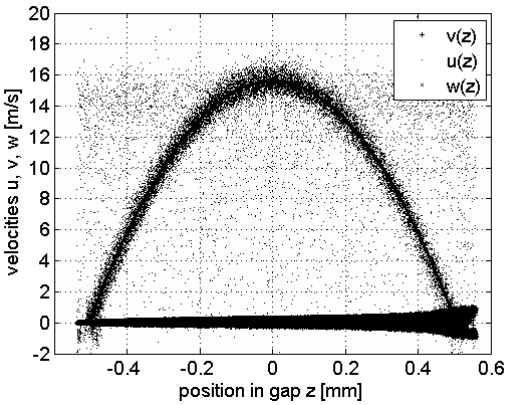

Fig. 14: Fitted from 50 snapshots (no. 270-319)

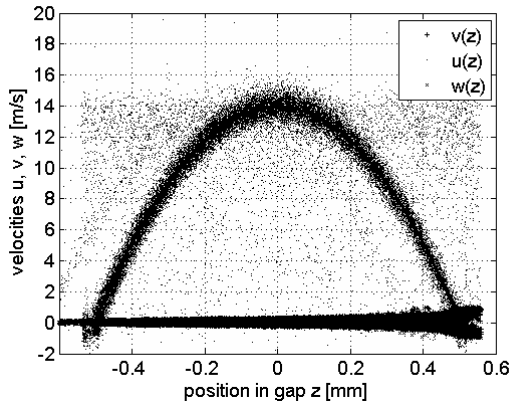

Fig. 15: Fitted from 100 snapshots (no. 100-199)

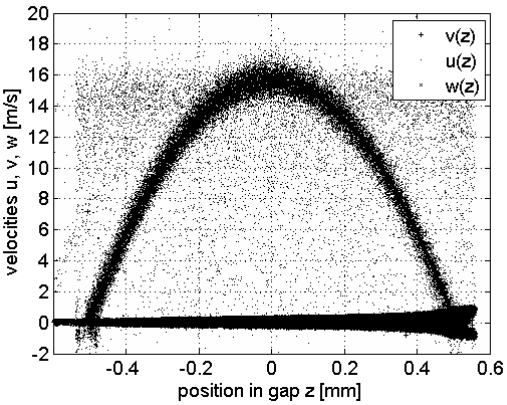

Fig. 16: Fitted from 100 snapshots (no. 251-350)

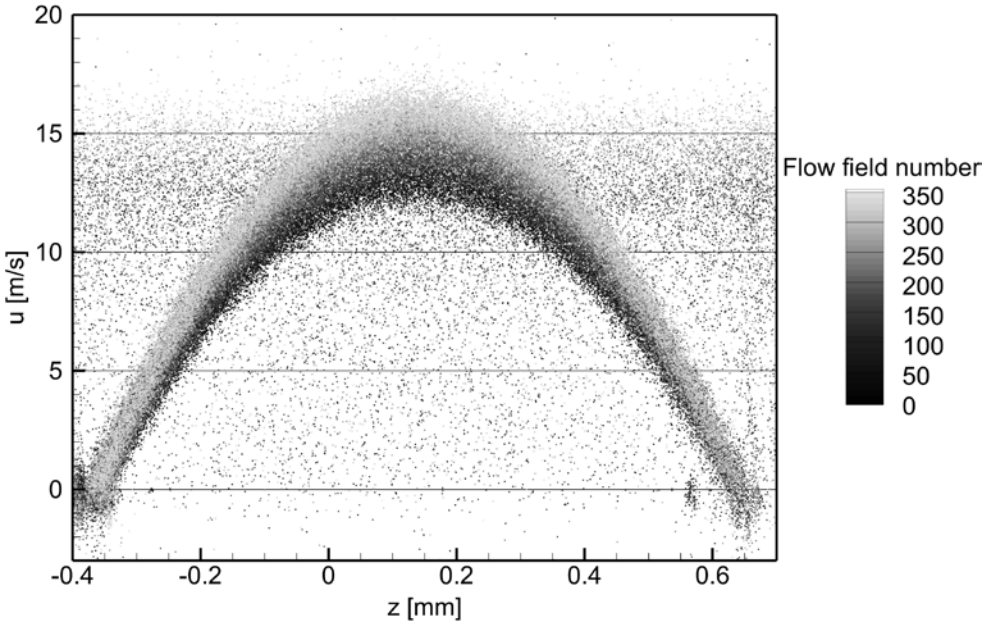

Fig. 17: All snapshots in one figure

In spite of the presence of noise (spurious displacements) in all charts of the analyzed data, the expected laminar velocity profile can be seen clearly. Even flow fields at a single time instance show the parabola very well. Nevertheless, there are still some difficulties to be mentioned:

Image processing still needs a lot of time. Fig. 7 shows an evaluated volume with a very low seeding density. This happens in less than 10% of all captured images. That is why the 2nd order polynomial function has not been fitted here. The displacements found in this case are still valid. The abnormality probably originates from the seeding generator, the pressure regulator or a disturbance in the supply pipe. Another possibility could be a temporarily illumination problem due to unnoticed vibration of the whole test rig or the laser beam. A computational evaluation problem can be excluded, because the raw images also show a comparatively low particle density.

In Fig. 17 it can be seen, that the maximum velocity is at the position z = +0.15 mm. This offset indicates a misalignment in the zero-millimeter-position between the calibration target and the front glass-plate. A tiny gap of 0.35 mm between the calibration target and the glass

plate can explain this discrepancy. During calibration using the DaVis 8.1.3, the front glass plate, hence the front wall should be at the zero-millimeter-position. In fact Fig. 17 shows the front wall at the position -0.35 mm. In Fig. 5 to 16 the zero *z*-positions are shifted back to the maximum velocity. The position of both walls can definitely be seen, due to the flow velocity at the wall of 0 m/s. The absolute value of the distance between the roots of the second degree polynomial has been calculated for every flow field. The deviation from the theoretical gap of 1 mm is lower than 1%. Furthermore a second parabola, shifted to the left of the original is visible in Fig. 13, which might be originated by reflections in the glass-plate, which affects the results of the tracking code.
Moreover, the maximum velocity is increasing when scanning along the 350 double-volumes, see Fig. 17. The reason for this change in velocity is that a quite simple pressure regulating valve was used for the measurments.
Fig. 5 to 16 show an increasing spread of the *v*- and *w*-velocity component with the *z*-position in the gap. A suitable explanation is difficult, but a reason for that might be an error in the alignment of both glass-plates. The wall in the positive *z*-direction is the rear glass-plate, which is the position of the maximum of this continuously increasing uncertainty. Also reflections on the surface and in the glass-plates, which restrict the validity of the particle tracking code, are possible explanations for that phenomenon. Moreover the illumination of the particles is very sensitive. Small changes in the mirror position (Fig. 1) lead to huge misalignments of the laser beam.

Conclusion and prospects

The feasibility study was successful, velocity profiles could be obtained in the 1 mm gap. Also, the experimental approach during this study led to an improved understanding of how to provide an appropriate illumination of the particles in the rotating disc test rig. The calibration procedure was shown to work properly. The contamination of the glass plates with DEHS particles requires the rotor to be removed for cleaning from time to time. All these facts have to be considered during the design process of the test rig. The transfer of the results of this stationary study to a rotating and vibrating test rig will be the next step.

Literature

Cierpka, C., Kähler, C. J., 2012: “Particle imaging techniques for volumetric three-component (3D3C) velocity measurements in microfluidics”, Journal of Visualization No. 15, pp. 1-31

Tesla, N., 1913: “Tesla Turbine,” U.S. Patent No. 1,061,206.

Nendl, D., 1976: “Dreidimensionale laminare Instabilitäten bei ebenen Wänden”, Zeitschrift für angewandte Mathematik und Mechanik (ZAMM) Nr. 56, T211-T213

Schlichting H., Gersten K., 2006: “Grenzschicht-Theorie”, 10th Edition, Springer-Verlag Berlin Heidelberg, p. 104

Hanks, R. W., Ruo, H. C., 1966: “Laminar-turbulent transition in ducts of rectangular cross section”, Industrial and Engineering Chemistry Fundamentals 5, pp. 558-568

Schade, H., Kunz, E., 1980: “Strömungslehre”, 2nd Edition, de Gruyter, p. 105